ON-MACHINE, IN-PROCESS, ULTRASONIC GAUGING AND FLAW DETECTION

Robert W. Reed

United Technologies
Research Center
East Hartford, CT. 06108

INTRODUCTION

An ultrasonic system has been assembled to provide real time thickness gauging on a lathe during a cutting operation. The same ultrasonic system provides flaw detection so that NDE of the part being machined is simultaneously accomplished. A key feature for good gauging performance is that the ultrasonic apparatus is configured to minimize sensitivity of the time interval measurements, used for the gauging operations, to variations in echo amplitude over a 30 dB dynamic range. Thickness data or flaw echo data can be displayed in a pseudo colored image format in near real time. The goal for this research is to make thickness measurements with an accuracy of better than 0.0005 in. over a minimum range of 0.1 to 1.0 in.

HARDWARE CONFIGURATION

Figure 1 shows the general arrangement of the apparatus. The transducer is mounted in a squirter assembly that is attached to a 5 axis positioner which is, in turn, permanently connected to the lathe carriage. The positioner thereby moves the squirter relative to the cutting tool position. Ordinary cutting fluid is used to couple the ultrasound to the part. The ultrasonic apparatus and the squirter motion controller are under full computer control. The computer/controller is a Hewlett Packard (HP) Model 330. It provides all data processing, image generation, and a continuous updated display of thickness statistics. The ultrasonic instrumentation is based on two modified MATEC MBS 8000 bin systems. An HP Model 5370B time interval counter can provide up to 6000 time interval measurements per second with single shot resolution of 20 ps. The peak sensing electronics provides a timing pulse to the counter that is referenced to the peak of the echoes used to start and stop the counter. The peak sensing electronics is the key feature that enables time interval measurements with typical rms deviations of 300 ps in the presence of echo amplitude variations of up to 30 dB. If unprocessed echoes are used as input to the counter, time interval measurement variations on the order of several hundred nanoseconds are typical for amplitude variations of this magnitude.

MATEC MBS 8000 bin systems are used for generating and receiving the ultrasound. They are fully computer controlled via an IEEE-488 bus. The gated peak detector (GPD) modules were modified to provide single shot peak detection. The original modules contained a single GPD that required 16 repetitions to reach the full peak value. However, each GPD module had complete delay and

Review of Progress in Quantitative Nondestructive Evaluation, Vol. 9
Edited by D.O. Thompson and D.E. Chimenti
Plenum Press, New York, 1990

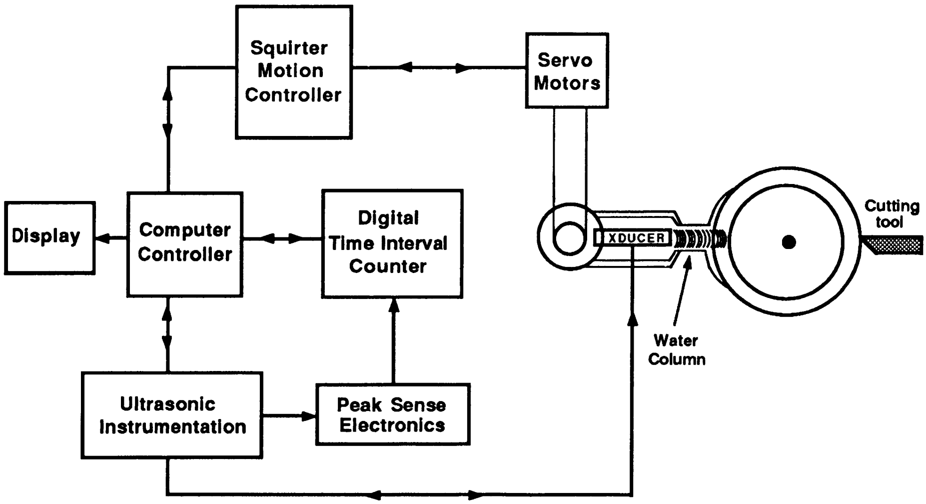

Figure 1. Gauging and flaw detection apparatus for use on a lathe.

gate circuitry for two peak detectors. The modified units contain dual peak detectors each capable of reading a peak value with a single sample. The gate signals for the peak detectors are provided as outputs. The peak detected amplitudes are output as analog signals which are input to the computer via a 16 channel A/D converter card manufactured by Infotek Systems.

Two MBS 8000 bins are used for the gauging and flaw detection operation. Figure 2 shows the arrangement of the Matec bins. The master bin contains in addition to a spike pulser, receiver and video detector, two dual GPD modules. The slave bin contains a receiver, video detector, stepless gate, and one dual GPD module. The master bin is externally triggered by a 1000 line shaft encoder attached to the lathe spindle. GPD #1 in the master bin detects the amplitude of the front surface echo (P_{1a}), detects the amplitude of internal flaw echoes (P_{1b}), and provides a gate signal (G_{1a}) to enable the peak sensing electronics for the front surface echo. The tracking trigger output from GPD #1 is used to trigger the slave bin. One gate output (G_{2a}) of GPD #2 is used to set the stepless gate in the slave bin to pass only the echo of interest to the receiver in the slave bin thereby eliminating receiver overload problems from the front surface echo when subsequent smaller echoes are amplified. The second gate (G_{2b}) of GPD #2 is set to a minimum width (50 ns) and delayed to occur 6 ms after the back surface echo of interest. This signal is fed into the slave bin receiver, along with the output of the stepless gate, to generate a missing echo signal with which to stop the time interval counter if the back echo should be missing. One gate output (G_{3b}) of GPD #3, which is in the slave bin, is used to enable the peak sensing electronics for the back surface echo and the missing echo trap signal.

The other channel of GPD #3 is used to detect the amplitude (P_{3a}) of the back surface echo but is set in width to not detect the following echo trap signal. All of the gate delays and widths are set by the computer software from input values of the thickness range to be monitored and the velocity of sound in the material. The general gate and GPD timing arrangement is shown in Fig. 3. The receiver gains are automatically set by the computer to provide good dynamic range. The transducer is automatically aimed to peak the echo signals.

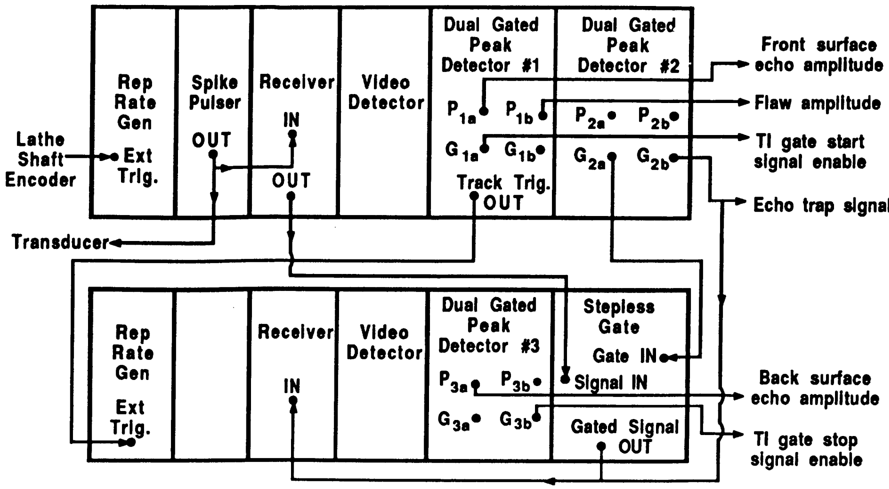

Figure 2. Ultrasonic hardware. Two modified Matec 8000 bin systems generate and receive all ultrasonic signals under full computer control.

CALIBRATION

The system is calibrated using 4 or more calibration blocks made of the same material as that being machined. Multiple blocks are used to calibrate both the velocity of sound in the material and to measure time delay differences in the echo signal paths through the electronic apparatus. The velocity and fixed time delay difference is used for all thickness calculations based on the time interval measurements made on the part being machined. The calibration blocks are mounted in an accessible and known location with regard to the allowable movements of the squirter assembly. The computer directs all movements of the squirter to the calibration blocks, automatically aims the transducer for best response, and acquires the time interval data for each block.

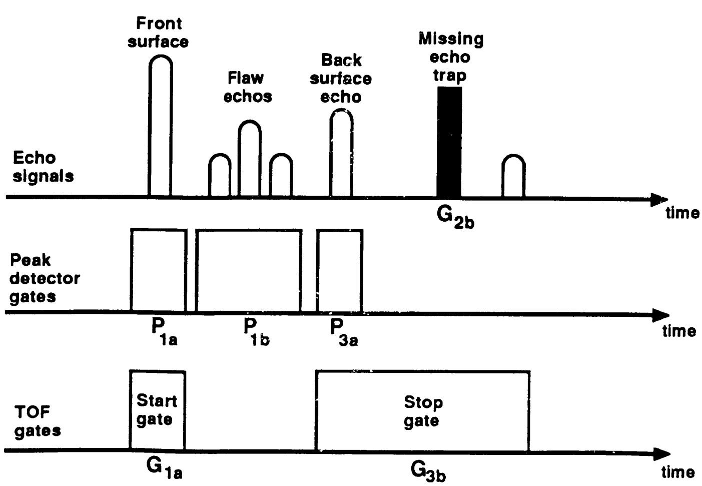

Figure 3. Signal timing for flaw detection and gauging. The synchronization between the ultrasonic echoes, gated peak detector timing, and start and stop gates for the time-of-flight measurements is shown.

EXAMPLE RESULTS

Example data were collected for two aluminum tubes during cutting operations. All data were acquired using a 15 MHz, unfocused, transducer. The wall thickness data typically has a resolution and repeatability of 0.0002 in. The absolute accuracy has not yet been fully calibrated. Measurements of the wall thickness, using calipers with 0.001 in. resolution are in agreement with the ultrasonic results. Better gauging apparatus is required to fully calibrate the ultrasonic results. In addition, the alloy type of the aluminum from which both the tubes and calibration blocks were constructed was unknown. More careful selection of the materials and better reference gauges will be required for full validation of the ultrasonic results.

4 in. O.D. Aluminum Tube

A 4 in. o.d. aluminum tube with a nominal 0.2 in. wall thickness was machined and gauged. Only the outside diameter was turned producing three distinct steps in the o.d. Four flat bottomed holes were cut into the tube from the inside in each of the two thicker regions.

Three holes were 0.063 in. and one 0.13 in. in diameter. The depths of the holes, which were used to simulate flaws, were unknown and different. All of the data shown for this tube were acquired after the final cutting operations were complete so that the three thickness regions, which were cut in separate operations, could be shown in one image.

Figure 4 is an image of the wall thickness of the tube with the horizontal direction being the circumference and the vertical dimension the length along the tube axis. The image contains 1000 data points in the circumferential direction and 250, separated by 0.008 in., along the axial direction. The aspect ratio is distorted since the 1000 points are determined by the lathe shaft encoder but the 0.008 in. separation is determined by the carriage feed rate along the lathe bed. The two horizontal stripes at the thickness step changes result from the finite beam width producing echoes from both thicknesses. This generates bad data which is flagged by the software and converted to the minimum thickness value permitted by the thickness range input by the operator at the start of the operation. The vertical striations in the image are from thickness changes resulting from extruder marks during the manufacture of the tube. Most of the flat bottomed holes are imaged but the depths are incorrect for one of two reasons. If the first hole echo falls in the stop gate width but the thickness lies outside the acceptable range it will be given the minimum thickness value by the computer. If the time interval circuitry is tripped by

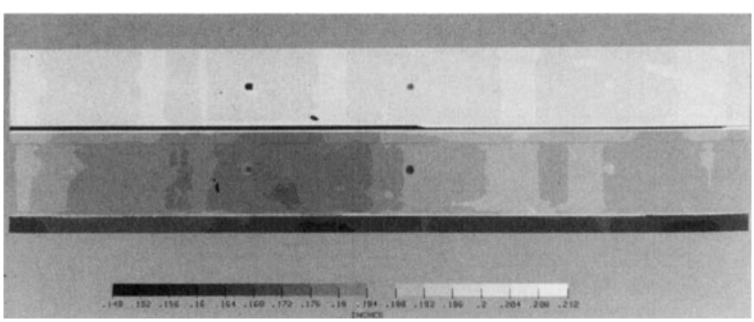

Figure 4. Wall thickness image for 2 in. long (vertical) section of 4 in. o.d. aluminum tube. A horizontal scan line contains 1000 points around the circumference of the tube.

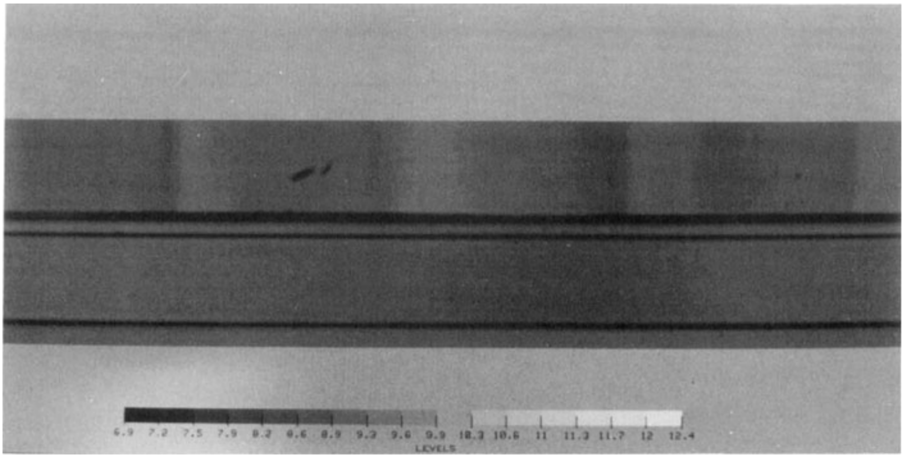

Figure 5. Front surface echo amplitude image for same tube section as Fig. 4.

one of the echo multiples, it could be imaged as a value within the thickness range.

Figure 5 is an image of the amplitude of the front surface echo. This image was acquired at the same time as the thickness data of Fig. 4. Two horizontal stripes in the image are from steps in the wall thickness which are on the squirter side of the tube wall. One noticeable surface blemish is obvious in the image and happens to be located right over a flat bottomed hole drilled from the back side. This will distort the image of the hole seen in subsequent figures. The middle horizontal stripe is from a surface groove. The upper part of this image, for the thicker part of the tube, is from an unmachined surface and shows more amplitude variation in general than for the machined surfaces.

Figure 6 is the amplitude of echoes, from "flaws", received by the peak detector gate P_{1b} of Fig. 3. The width of the gate is not as wide as the total thickness of the part. Hence, very shallow flaws can be missed. Three of the four flat bottomed holes, in each of the two thickest regions, show up as higher amplitude echoes. The fourth, very shallow, hole in each region is missed in this image. The 0.063 and 0.13 in. dia. holes are distinguishable in size.

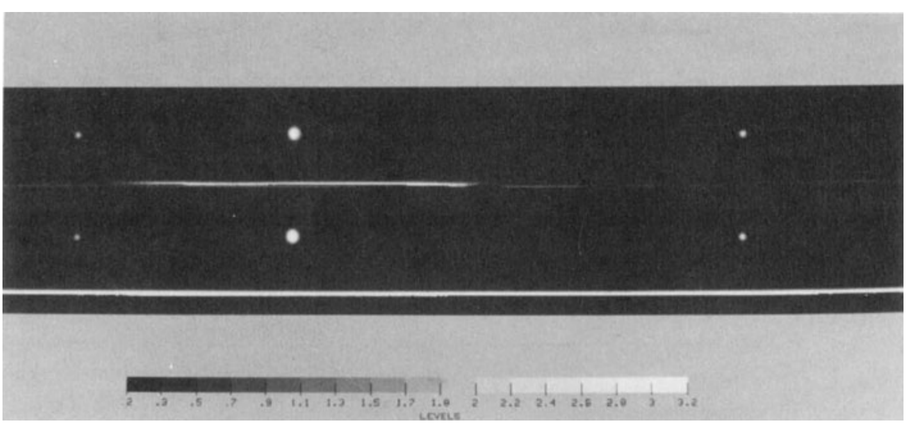

Figure 6. Internal flaw echo amplitude image for same tube section as Fig. 4.

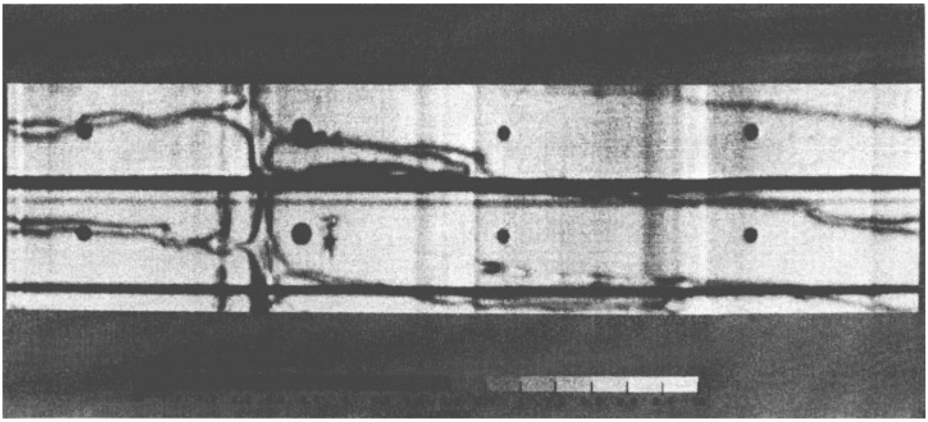

Figure 7. Back surface echo amplitude image for same tube section as Fig. 4.

Figure 7 is an image of the back (inside) surface echo. All flat bottomed holes now show up as a lack of back surface echo amplitude. The front surface blemish seen in Fig. 5 also diminishes the back surface echo and shows up as a distortion of the larger hole in the top thickness layer of the image. The large vertical features result from extruder marks on the inside surface. The more random nearly horizontal features are apparently due to cutting fluid rolling on the inside of the tube. Note that these amplitude variations don't affect the thickness measurements as displayed in Fig. 4.

<u>2.8 in. O.D. Aluminum Tube</u>

An aluminum tube was machined on both the outside and inside while it was being gauged. The tube was not perfectly centered in the chuck so that the first o.d. cutting operation produced an outside surface that was not concentric with the inside. After the inside was subsequently machined, the surfaces were again concentric.

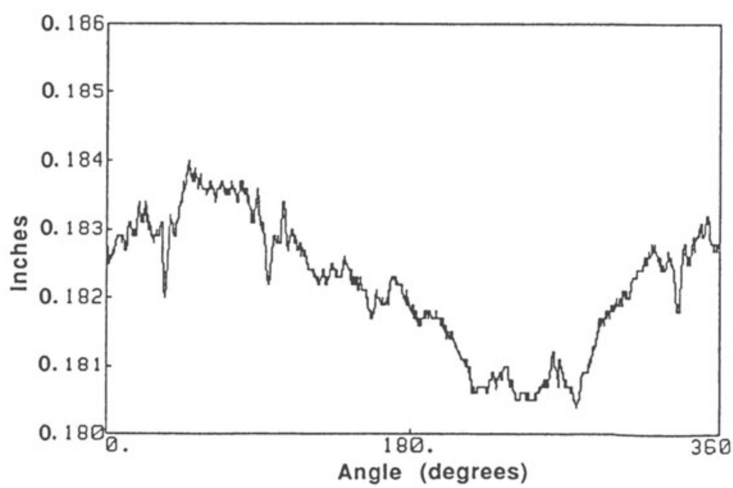

Figure 8. Thickness for one circumferential section of 2.8 in. o.d. tube before cutting.

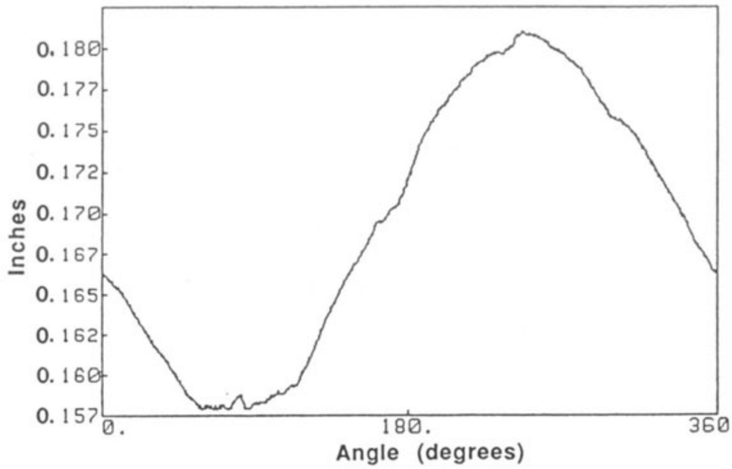

Figure 9. Thickness for one circumferential section of 2.8 in. o.d. tube after cutting the outside surface.

Figure 8 is an example of the thickness of the tube around the circumference before the first cut was made. The graphic plot is shown, rather than an image of a length of tube since more detail can be graphically presented than with a 16 level grey scale image. The overall variation about the circumference is verifiable with a mechanical caliper. The smaller features are completely repeatable on subsequent ultrasonic gauging operations.

Figure 9 is a plot of the thickness obtained as the o.d. was cut. Note the large variation in thickness resulting from the nonconcentricity. The thickness range, 0.023 in., is much larger than for Fig. 8 with the result that small details are no longer evident.

Figure 10 is an image of the thickness for a 2 in. length (vertical dimension) of the tube. The concentricity is seen to vary along the length.

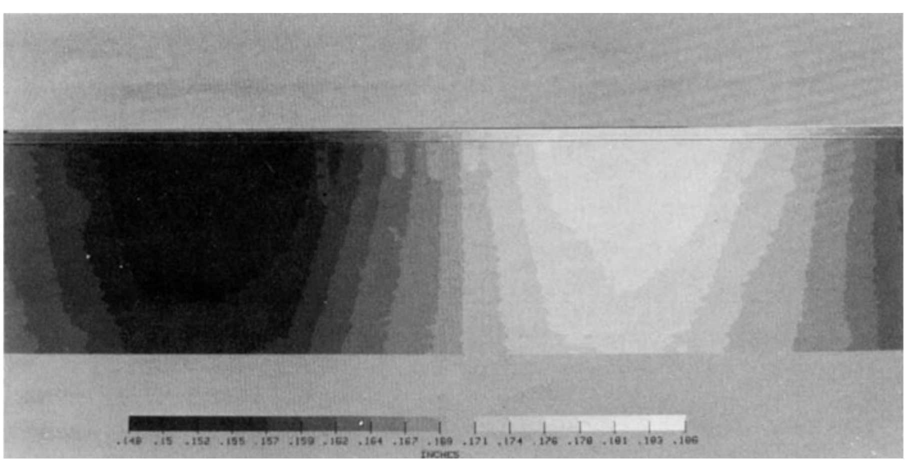

Figure 10. Thickness image of 2 in. length of tube from which Fig. 9 data was extracted.

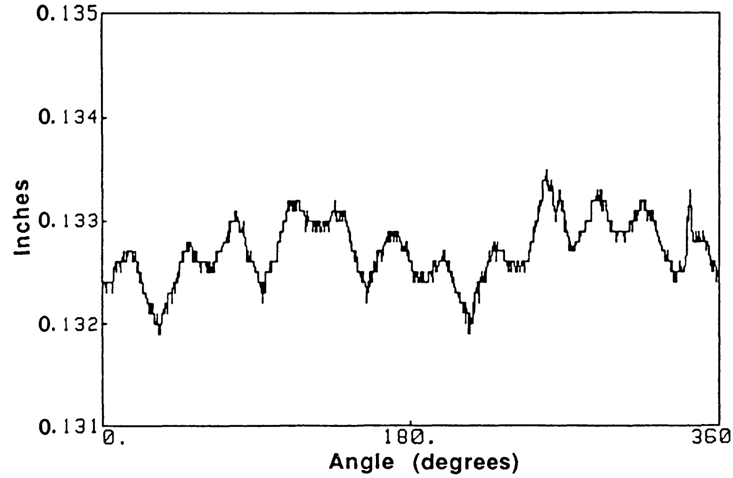

Figure 11. Thickness for one circumferential section of 2.8 in. o.d. tube after an inside cut which followed the cut that produced Fig. 9.

Figure 11 is an example plot of the thickness after the i.d. was cut. Most of the nonconcentricity has now been removed. All of the details of this plot are repeatable. The total range of the data is now less than 0.002 in.

CONCLUSIONS

On-machine, in-process, ultrasonic thickness gauging and flaw detection have been demonstrated. Sensitivity of the thickness measurements to echo amplitude variations are much smaller than for standard ultrasonic thickness gauges. Typical time interval rms deviations for the time interval measurements are approximately 300 ps. For most metallic sound velocities this gives a measurement precision on the order of 0.0001 in.

More careful metrological verifications of the thickness measurements must be carried out. Careful selection of the calibration block material must be made to be certain that it is representative of the material being cut.

Efforts will be undertaken in the future to implement the surface finish measurement techniques developed at NIST [1]. These measurements involve measurement of the echo amplitude. Such data is readily available from the current system configuration. Hence, implementation of the NIST methods will only require software development.

REFERENCE

1. G. V. Blessing, P. P. Bagley, and J. E. James, The Effect of Surface Roughness on Ultrasonic Echo Amplitude in Steel, Materials Evaluation, 42, pp. 1389-1400, (1984).